planes,[26] and strength of bridging bonds.[19] High planarity in oxime-bridged (Cu–O–N–Cu) dimers has been shown to provide strong coupling.[27] Features remote from the metal bridging framework such as ring substituents on ligand phenyl rings were found to be relatively unimportant, in general.[22-25] The most prominent structural difference in the bridging geometries of [Cu$_3$OH(ClO$_4$)]ClO$_4$ and [Cu$_3$OL'$_3$(ClO$_4$)]$_2$ is the tetrahedral oxygen coordination (sp^3) in the Cu$_3$OH complex and the nearly planar configuration (sp^2) in Cu$_3$O. Another important structural difference is the higher degree of coplalarity of the three principal ligand planes in the Cu$_3$O complex than in the Cu$_3$OH complex: in Cu$_3$OH, these three planes [O, O(A), N(1A), N(2A); O, O(B), N(1B), N(2B); O, O(C), N(1C), N(2C)] make angles of 40.3, 28.5, and 31.1° with each other, while in Cu$_3$O the angles are only 14.6, 20.4, and 26.6°. Thus, [Cu$_3$OL'$_3$(ClO$_4$)]$_2$ approaches more closely to the strongly antiferromagnetic planar oxime-bridged binuclear copper(II) complexes. A minor structural difference is the higher degree of coplanarity of the metal atoms with the ONCCN ligand planes in the Cu$_3$O complex (Cu atoms out of plane by 0.09 Å on the average; only Cu(C), which provides the intertrimer bridge, is markedly out of plane at 0.18 Å) than in the Cu$_3$OH complex (average 0.16 Å). This change in skeletal geometry can readily explain the difference in magnetic behavior between the two complexes.

The Cu$_3$OH complex has weaker magnetic exchange ($J = -122$ cm^{-1}). The tetrahedral sp^3 hybridization forces the oxygen above the plane of the copper atoms and furthermore disrupts the coplanar oxime-bridging network due to the hindered d$_{x^2-y^2}$ overlap. The nonplanar bonding configuration is achieved at the expense of magnetic-exchange stabilization.

The Cu$_3$O complex on the other hand has nearly coplanar geometry; the Cu$_3$O oxygen is only slightly raised above the plane to form a weak intertrimer bond. As a result of the nearly coplanar configuration plus additional electrostatic effects, the Cu–O bonds are shorter for the Cu$_3$O complex. Since the oxygen exhibits the more flat sp^2 character, overlap with the copper d$_{x^2-y^2}$ orbitals still permits the oxime ligands to retain their coplanar geometry. This overall coplanar Cu$_3$OL'$_3$ structure permits larger magnetic exchange ($J \geq 300$ cm^{-1}).

Acknowledgment. Support under NSF Grant No. CHE77-01372 is gratefully acknowledged.

Registry No. **1**, 75701-18-7; **2**, 75701-19-8; butane-2,3-dione oxime, 57-71-6; benzil oxime, 14090-77-8; aniline, 62-53-3; methylamine, 74-89-5.

Supplementary Material Available: Tables of least-squares planes and observed and calculated structure factors (30 pages). Ordering information is given on any current masthead page.

---

(21) Gluvchinsky, P.; Mockler, G. M.; Healy, P. C.; Sinn, E. *J. Chem. Soc., Dalton Trans.* **1974**, 1156.

(22) Countryman, R. M.; Robinson, W. T.; Sinn, E. *Inorg. Chem.* **1974**, *13*, 2013.

(23) Sinn, E. *J. Chem. Soc., Chem. Commun.* **1975**, 665; *Inorg. Chem.* **1976**, *15*, 358.

(24) Davis, J. A.; Sinn, E. *J. Chem. Soc., Dalton Trans.* **1976**, 165.

(25) Butcher, R. J.; Sinn, E. *Inorg. Chem.* **1976**, *15*, 1604.

(26) Sinn, E. *Inorg. Chem.* **1976**, *15*, 2698.

(27) Butcher, R. J.; O'Connor, C. J.; Sinn, E. *Inorg. Chem.* **1979**, *18*, 1913 and references cited.

Contribution from the Departments of Chemistry, Universtiy of New Orleans, New Orleans, Louisiania 70122, and University of Virginia, Charlottesville, Virginia 22901

Crystal Structures and Magnetic Properties of Cobalt(II) Pyrazinecarboxylate and Pyrazinedicarboxylate Complexes

CHARLES J. O'CONNOR[1a] and EKK SINN*[1b]

Received May 8, 1980

The synthesis and the structural and magnetic characterization of three cobalt(II) complexes of 2-pyrazinecarboxylic acid and 2,3-pyrazinedicarboxylic acid are reported. In each case the cobalt is in a distorted octahedral environment, coordinated to two nitrogen atoms and two carboxylate oxygens from different ligands and two water molecules. Pairs of like ligands are always trans to each other. The pyrazine ligands do not link adjacent cobalt atoms directly. The complexes all consist of three-dimensionally hydrogen-bonded polymers with potential magnetic-exchange pathways. In [Co(pz(COO)COOH)$_2$(H$_2$O)$_2$], the carboxylate group at the 2-position is deprotonated, while the other carboxylate forms intramolecular hydrogen bonds with it and intermolecular hydrogen bonds with the coordinated water. In [Co(pzCOO)$_2$(H$_2$O)$_2$], the coordinated carboxylate oxygen is hydrogen bonded to the coordinated water of adjacent molecules. This causes lengthening of the Co–O bond to the carboxylate and forms infinite chains along the *a* axis. It is the most direct linkage observed in the three complexes. The remainder of the three-dimensional network is formed by hydrogen bonding between the uncoordinated carboxylate oxygen and the coordinated water molecule. In [Co(pzCOO)$_2$(H$_2$O)$_2$]·2H$_2$O, the uncoordinated carboxylate groups form infinite chains along the *a* axis by hydrogen bonding to the coordinated water ligands of adjacent molecules. The remainder of the three-dimensional network is less direct, being completed by uncoordinated water molecules hydrogen bonding to both the uncoordinated carboxylate oxygens and coordinated water molecules of adjacent molecules. Powder magnetic susceptibilities were measured on each of the cobalt pyrazinecarboxylate complexes in the region 4–100 K. The low-temperature behavior of the Kramers doublet of cobalt(II) may be analyzed by the Curie–Weiss law. This procedure gives a Weiss constant of about $\Theta \approx -1.0$ K for each of the complexes. The small negative value of J is indicative of weak antiferromagnetic interactions, with critical regions below the temperature range of measurement. Crystal data for [Co(pz(COO)COOH)$_2$(H$_2$O)$_2$]: space group $P2_1/n$, $Z = 4$, $a = 9.396$ (3) Å, $b = 7.692$ (2) Å, $c = 10.136$ (2) Å, $\beta = 93.32$ (4)°, $V = 731$ Å^3, $R = 3.2\%$ for 1225 reflections. Crystal data for [Co(pzCOO)$_2$(H$_2$O)$_2$]·2H$_2$O: space group $P2_1/n$, $Z = 4$, $a = 7.259$ (3) Å, $b = 13.028$ (3) Å, $c = 8.271$ (5) Å, $\beta = 103.09$ (3)°, $V = 765$ Å^3, $R = 3.1\%$ for 1195 reflections. Crystal data for [Co(pzCOO)(H$_2$O)$_2$]: space group $P2_1/n$, $Z = 4$, $a = 5.2496$ (7) Å, $b = 11.140$ (1) Å, $c = 10.299$ (2) Å, $\beta = 99.55$ (1)°, $V = 594$ Å^3, $R = 2.2\%$ for 997 reflections.

Introduction

Pyrazine, when coordinated to transition metals, is an excellent bridging ligand.[2-12] It allows electron coupling between the metals via orbital overlap with the ligand orbitals[2-7] and is therefore a potential transmitter of magnetic-exchange in-

---

(1) (a) University of New Orleans. (b) University of Virginia.

(2) Creutz, C.; Taube, H. *J. Am. Chem. Soc.* **1969**, *91*, 3988; **1973**, *95*, 1086.

teractions.[9-12] Carboxylate ligands are equally capable of bridging and providing exchange pathways when paramagnetic metals are involved. For example, they form binuclear complexes with Cu(II),[13-15] Cu(I),[16] Co(II),[17,18] Rh(II),[19,20] Cr(II),[21] Mo(II),[22,23] Pd(II),[24] Ru(II),[25] and Ni(II)[26] by bonding by one oxygen atom to each metal, to form a three-atom bridge, or even by bonding with a single oxygen atom to two metals to form a one-atom bridge.[27] Here we combine the bridging groups by using pyrazinecarboxylates with cobalt(II). A related ligand, pyridine-2,6-dicarboxylate, forms binuclear Cr(III) complexes in which OH ligands form the Cr–O–Cr bridge.[28]

In this work, we have synthesized an unusual series of cobalt(II) complexes in which pyrazinecarboxylate and pyrazinedicarboxylate act as nonbridging chelating ligands, forming CoL_2 monomeric units. The orientation of the pyrazine ligands is of interest for purely chemical bonding considerations. There are reports of many pyrazine-bridged, magnetically coupled systems, and for these complexes the most favorable orientation places the bridging plane perpendicular to the coordination plane.[9-12] The complexes reported here provide an opportunity to investigate nonbridging bonding orientations.

From the results of the crystal structure, the mononuclear units are bridged by hydrogen bonds through the pyrazinecarboxylate ligands. The analysis of the magnetic data shows the interaction to be small and antiferromagnetic ($\Theta \approx -1.0$ K).

We report on the X-ray crystal structures and variable-temperature (4–100 K) powder magnetic susceptibilities for the complexes $CoL_2 \cdot nH_2O$, where HL = 2,3-pyrazinedicarboxylic acid ($n = 2$) and pyrazinecarboxylic acid ($n = 2$, 4).

Experimental Section

Preparation of the Complexes. $[Co(pz(COO)COOH)_2(H_2O)_2]$ and $[Co(pzCOO)_2(H_2O)_2] \cdot 2H_2O$. A 5-mmol sample of the pyrazinecarboxylate was dissolved in 150 mL of H_2O. A 2.5-mmol sample of cobalt(II) chloride was dissolved in 25 mL of H_2O. The solutions were mixed, and single crystals suitable for X-ray analysis were deposited after the solutions were allowed to stand overnight. For **$[Co(pzCOO)_2(H_2O)_2]$** the amounts and solution volumes are the same as above; however 1 M $HClO_4$ was used in place of water and cobalt(II) perchlorate was used in place of cobalt(II) chloride.

Crystal Data for $[Co(pz(COO)COOH)_2(H_2O)_2]$: $CoO_{10}N_4C_{12}H_{10}$, mol wt 427, space group $P2_1/n$, $Z = 4$, $a = 9.396$ (3) Å, $b = 7.692$ (2) Å, $c = 10.136$ (2) Å, $\beta = 93.32$ (4)°, $V = 731$ Å^3, $\rho_{calcd} = 1.95$ g cm^{-3}, $\rho_{obsd} = 1.949$ g cm^{-3}, μ(Mo Kα) = 13.0 cm^{-1}; crystal dimensions (distances in mm of faces from centroid) $(10\bar{1})$ 0.30, $(\bar{1}01)$ 0.30, (101) 0.135, $(\bar{1}0\bar{1})$ 0.135, $(1\bar{1}0)$ 0.27, $(\bar{1}10)$ 0.27, (110) 0.30, $(\bar{1}\bar{1}0)$ 0.30, $(0\bar{1}1)$ 0.275; maximum, minimum transmission coefficients 0.69, 0.61.

Crystal Data for $[Co(pzCOO)_2(H_2O)_2] \cdot 2H_2O$: $CoO_8N_4C_{10}H_{14}$, mol wt 377, space group $P2_1/n$, $Z = 4$, $a = 7.259$ (3) Å, $b = 13.028$ (3) Å, $c = 8.271$ (5) Å, $\beta = 103.09$ (3)°, $V = 765$ Å^3, $\rho_{calcd} = 1.64$ g cm^{-3}, $\rho_{obsd} = 1.68$ g cm^{-3}, μ(Mo Kα) = 12.2 cm^{-1}; crystal dimensions (mm from centroid) (100) 0.18, $(\bar{1}00)$ 0.18, (010) 0.16, $(0\bar{1}0)$ 0.16, (011) 0.14, $(0\bar{1}\bar{1})$ 0.14, $(01\bar{1})$ 0.10, $(0\bar{1}1)$ 0.10; maximum, minimum transmission coefficients 0.85, 0.78.

Crystal Data for $[Co(pzCOO)_2(H_2O)_2]$: $CoO_6N_4C_{10}H_{10}$, mol wt 341, space group $P2_1/c$, $Z = 4$, $a = 5.2496$ (7) Å, $b = 11.140$ (1) Å, $c = 10.299$ (2) Å, $\beta = 99.55$ (1)°, $V = 594$ Å^3, $\rho_{calcd} = 1.92$ g cm^{-3}, $\rho_{obsd} = 1.90$ g cm^{-3}, μ(Mo Kα) = 15.4 cm^{-1}; crystal dimensions (mm from centroid) (100) 0.21, $(\bar{1}00)$ 0.21, (011) 0.155, $(0\bar{1}\bar{1})$ 0.155, $(01\bar{1})$ 0.155, $(0\bar{1}1)$ 0.155, (001) 0.155, $(00\bar{1})$ 0.155; maximum, minimum transmission coefficients 0.80, 0.67.

Cell dimensions and space group data were obtained by standard methods on an Enraf-Nonius four-circle CAD-4 diffractometer. The θ–2θ scan technique was used, as previously described,[29] to record the intensities for all nonequivalent reflections for which $1° < 2\theta < 50°$ for all three crystals. Scan widths were calculated as ($A + B \tan \theta$), where A is estimated from the mosaicity of the crystal and B allows for the increase in width of peak due to Kα_1–Kα_2 splitting. The values of A and B were 0.6 and 0.35°, respectively, for $[Co(pz(COO)COOH)_2(H_2O)_2]$ and $[Co(pzCOO)_2(H_2O)_2]$ and 0.5 and 0.35°, respectively, for $[Co(pzCOO)_2(H_2O)_2] \cdot 2H_2O$.

The intensities of four standard reflections, monitored for each crystal at 100-reflection intervals, showed no greater fluctuations than those expected from Poisson statistics. The raw intensity data were corrected for Lorentz–polarization effects and absorption. Of the 1279 independent intensities for $[Co(pz(COO)COOH)_2(H_2O)_2]$, 1305 for $[Co(pzCOO)_2(H_2O)_2] \cdot 2H_2O$, and 1017 for $[Co(pzCOO)_2(H_2O)_2]$, there were 1225, 1195, and 997 for the three complexes respectively, with $F_o^2 > 3\sigma(F_o^2)$, where $\sigma(F_o^2)$ was estimated from counting statistics.[30] These data were used in the final refinement of the structural parameters.

Structure Determinations. For $[Co(pz(COO)COOH)_2(H_2O)_2$, several factors made the location of the cobalt atom on a special position, the origin, seem reasonably likely: the unit cell size, combined with an assumed approximate nonhydrogen atom volume of about 18 Å^3, the reflection intensities, the suspected polymeric nature of the structure which would permit an origin-centered monomeric subunit, and the lack of any strong cobalt–cobalt vectors on the origin-removed Patterson calculated from all intensity data. Solution of the structure then resulted from the interpretation of the strongest Patterson vectors as cobalt–light atom peaks. The model was confirmed by the subsequent solution of the structure. The positions of all the hydrogen and nonhydrogen atoms were determined from Fourier syntheses.

The same factors governed a similar choice for the cobalt positions in the other two complexes. The solution proceeded as before. All atoms including hydrogens were located. A hydrogen-bonding polymeric structure was evident in each case. Full-matrix least-squares refinement was carried out as previously described.[29]

Anisotropic temperature factors were then introduced for all nonhydrogen atoms, and after refinement of the models, the hydrogen parameters were included in the refinement for two cycles and subsequently held fixed. The models converged with $R = 3.2\%$ and $R_w = 4.8\%$ for $[Co(pz(COO)COOH)_2(H_2O)_2]$, $R = 3.1\%$ and $R_w = 5.0\%$

---

(3) Beattie, J. K.; Hush, N. S.; Taylor, P. R. *Inorg. Chem.* **1976**, *15*, 992.
(4) Meyer, T. J.; Powers, M. J.; Salmon, D. J.; Callahan, R. W. *J. Am. Chem. Soc.* **1977**, *99*, 1064.
(5) Meyer, T. J. *Acc. Chem. Res.* **1978**, *11*, 94.
(6) Baumann, J. A.; Salmon, D. J.; Wilson, S. T.; Meyer, T. J. *Inorg. Chem.* **1979**, *18*, 2472.
(7) Carreck, P. W.; Goldstein, M.; McPartlin, E. M.; Unsworth, W. D. *J. Chem. Soc. D* **1971**, 1634.
(8) Inoue, M.; Kubo, M. *Coord. Chem. Rev.* **1976**, *21*, 1.
(9) Richardson, H. W.; Wasson, J. R.; Hatfield, W. E. *Inorg. Chem.* **1977**, *16*, 484.
(10) Blake, A. B.; Hatfield, W. E. *J. Chem. Soc., Dalton Trans.* **1978**, 863.
(11) Haddad, M. S.; Hendrickson, D. N.; Cannady, J. P.; Drago, R. S.; Biecksza, D. S. *J. Am. Chem. Soc.* **1979**, *101*, 898.
(12) Darriet, J.; Haddad, M. S.; Duesler, E. N.; Hendrickson, D. N. *Inorg. Chem.* **1979**, *18*, 2679.
(13) Van Niekerk, J. H.; Schoenig, F. R. L. *Acta Crystallogr.* **1953**, *6*, 227.
(14) Doedens, R. J. *Prog. Inorg. Chem.* **1976**, *21*, 209 and references cited.
(15) Sinn, E. *Coord. Chem. Rev.* **1970**, *5*, 313 and references cited.
(16) Drew, M. G. B.; Edwards, D. A.; Richards, R. *J. Chem. Soc., Dalton Trans.* **1977**, 299.
(17) Catterick, J.; Hursthouse, M. B.; Thornton, P.; Welch, A. J. *J. Chem. Soc., Dalton Trans.* **1977**, 223 and references cited.
(18) Drew, J.; Hursthouse, M. B.; Thornton, D.; Welch, A. J. *J. Chem. Soc., Chem. Commun.* **1973**, 52.
(19) Cotton, F. A.; Felthouse, T. R. *Inorg. Chem.* **1980**, *19*, 323.
(20) Aoki, K.; Yamazaki, H. *J. Chem. Soc., Chem. Commun.* **1980**, 186.
(21) Cotton, F. A.; deBoer, B. G.; La Prade, M. D.; Pipal, J. R.; Ucko, D. A. *Acta Crystallogr., Sect. B* **1971**, *B27*, 1664.
(22) Cotton, F. A.; Norman, J. G., Jr. *J. Am. Chem. Soc.* **1972**, *94*, 5697.
(23) Clegg, W.; Garner, C. D.; Parkes, S.; Walton, I. B. *Inorg. Chem.* **1979**, *18*, 2250.
(24) Churchill, M. R.; Mason, R. *Nature (London)* **1964**, *204*, 777.
(25) Bino, A.; Cotton, F. A.; Felthouse, T. R. *Inorg. Chem.* **1979**, *18*, 2599.
(26) Butcher, R. J.; O'Connor, C. J.; Sinn, E., *Inorg. Chem.*, in press.
(27) Butcher, R. J.; Overman, J. W.; Sinn, E. *J. Am. Chem. Soc.* **1980**, *102*, 3276.
(28) Cline, S. J.; Kallesøe, S.; Pedersen, E.; Hodgson, D. J. *Inorg. Chem.* **1979**, *18*, 796.
(29) Freyberg, D. P.; Mockler, G. M.; Sinn, E. *J. Chem. Soc., Dalton Trans.* **1976**, 447.
(30) Corfield, P. W. R.; Doedens, R. J.; Ibers, J. A. *Inorg. Chem.* **1967**, *6*, 197.

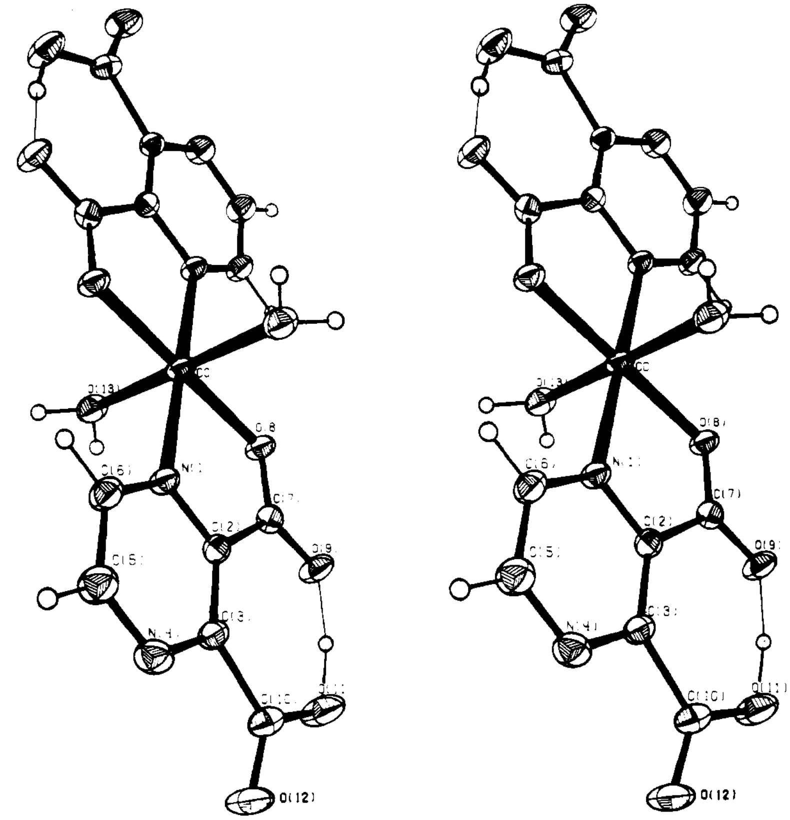

Figure 1. Stereopair view of $[Co(pz(COO)COOH)_2(H_2O)_2]$.

for $[Co(pzCOO)_2(H_2O)_2]\cdot 2H_2O$, and $R = 2.2\%$ and $R_w = 3.1\%$ for $[Co(pzCOO)_2(H_2O)_2]$. A final Fourier difference function was featureless. Tables of the observed and calculated structure factors are available.[31] The principal programs used are as previously described.[29]

Magnetic Measurements. Magnetic susceptibilities were measured on a superconducting susceptometer from 4 to 100 K. The calibration of the instrument and measurement techniques are described elsewhere.[32,33]

Results and Discussion

Final positional and thermal parameters for $[Co(pz(COO)COOH)_2(H_2O)_2]$, $[Co(pzCOO)_2(H_2O)_2]\cdot 2H_2O$, and $[Co(pzCOO)_2(H_2O)_2]$ are given in Table I. Tables II–IV contain the bond lengths and angles. The digits in parentheses in the tables are the estimated standard deviations in the least significant figures quoted and were derived from the inverse matrix in the course of least-squares refinement calculations. Figure 1 shows a stereopair view of the $[Co(pz(COO)COOH)_2(H_2O)_2]$ molecule while Figure 2 shows the hydrogen-bonding network in the unit cell lattice. The hydrogen atom positions show that each of the two carboxylate groups in $[Co(pz(COO)COOH)_2(H_2O)_2]$ share a single proton, which is closer to the O(11) of the uncoordinated carboxylate than to O(9). Each coordinated water molecule is hydrogen bonded to the uncoordinated carboxylate O(12) atom of four different molecules, to form a three-dimensional hydrogen-bonded network. The intermolecular hydrogen bonding is clearly suitable as a magnetic-exchange pathway. Linkages via O(12)–H(131)–O(13) connect the parallel to the *a* axis, while the remaining network is via O(12)–H(132)–O(13).

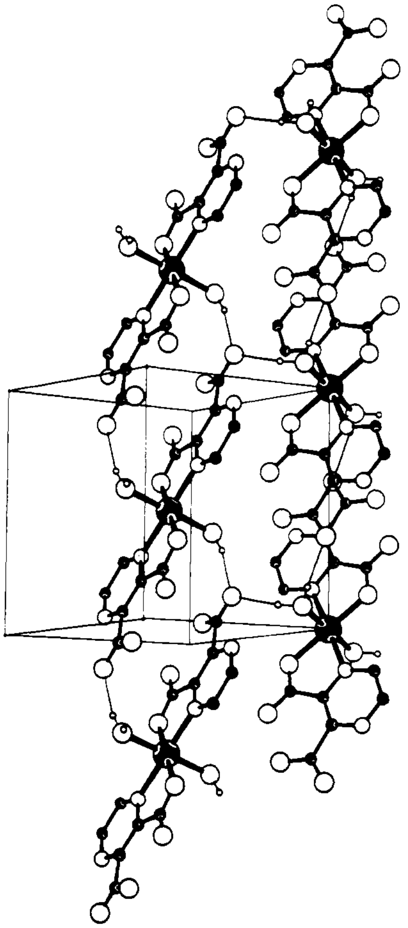

Figure 2. Molecular packing in $[Co(pz(COO)COOH)_2(H_2O)_2]$, showing part of the hydrogen-bonded network.

Figure 3 shows a stereopair view of the $Co(pzCOO)_2(H_2O)_2]$. Figures 4 and 5 show the hydrogen-bonding networks in $[Co(pzCOO)_2(H_2O)_2]\cdot 2H_2O$ and $[Co(pzCOO)_2(H_2O)_2]$, respectively. In the $Co(pzCOO)_2(H_2O)_2$ lattice,

---

(31) Supplementary material.

(32) O'Connor, C. J.; Sinn, E.; Cukauskas, E. J.; Deaver, B. S., Jr. *Inorg. Chim. Acta* **1979**, *32*, 29.

(33) Bucelot, T. J.; Galfo, C.; Farris, T.; Deaver, B. S., Jr., O'Connor, C. J.; Sinn, E., to be submitted for publication.

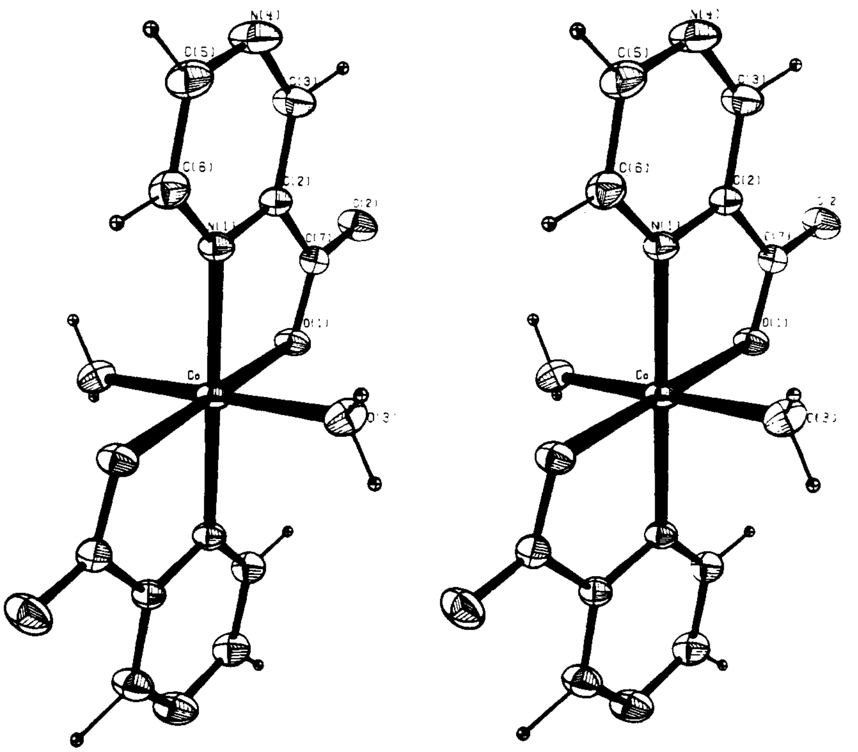

Figure 3. Stereopair view of $[Co(pzCOO)_2(H_2O)_2]$. Essentially the same central molecular unit exists in $[Co(pzCOO)_2(H_2O)_2]\cdot 2H_2O$.

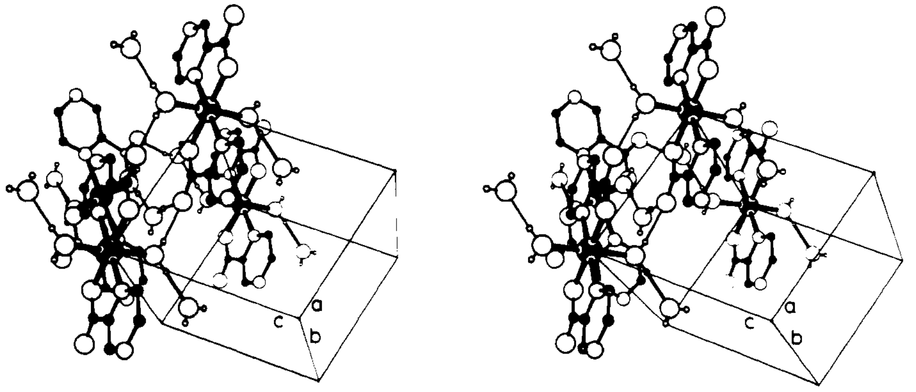

Figure 4. Molecular packing in $[Co(pzCOO)_2(H_2O)_2]\cdot 2H_2O$, showing part of the hydrogen-bonded network.

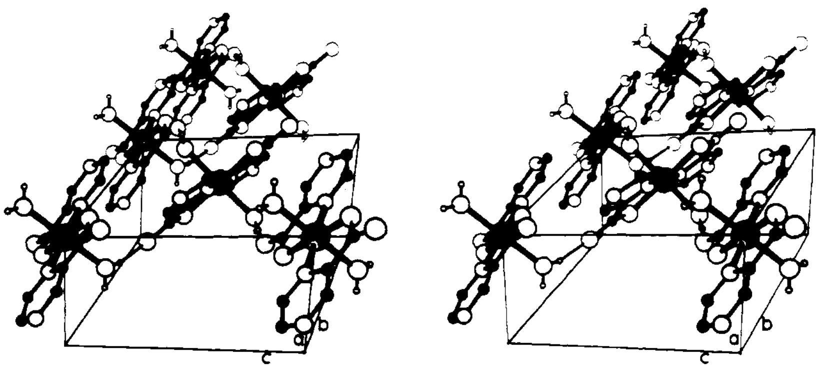

Figure 5. Molecular packing in $[Co(pzCOO)_2(H_2O)_2]$, showing part of the hydrogen-bonded network.

hydrogen-bonding linkages O(1)–H(10)–O(3), via the hydrogen atoms of the coordinated water molecule, form chains parallel to the *a* axis. Hydrogen-bonding linkages, O(2)–H(20)–O(3), also via coordinated water molecules, complete a three-dimensional network. The intermolecular hydrogen bonding is suitable as a magnetic-exchange pathway. The magnetically most direct linkage is parallel to the *a* axis because it involves hydrogen bonding between oxygen atoms coordinated directly to the metal atoms on neighboring molecules. This is the most direct linkage observed in the three compounds. The hydrogen bonding to the coordinated carboxylate oxygen appears to cause a slight lengthening of the Co–O bond to the carboxylate. This bond is 2.093 (1) Å, compared with values of 2.057 (1) and 2.084 (1) Å for $[Co(pz(COO)COOH)_2(H_2O)_2]$ and $[Co(pzCOO_2(H_2O)_2]\cdot 2H_2O$, respectively.

Table I. Positional and Thermal Parameters and Their Estimated Standard Deviations[a]

(a) $[Co(C_4N_2(COO)COOH)_2(H_2O)_2]$

atom	x	y	z	B_{11}	B_{22}	B_{33}	B_{12}	B_{13}	B_{23}
Co	0.0000 (0)	0.0000 (0)	0.0000 (0)	1.13 (1)	1.61 (1)	1.97 (1)	−0.145 (8)	0.67 (1)	−0.070 (9)
O(8)	0.1363 (1)	−0.1726 (2)	−0.0828 (1)	1.48 (4)	1.78 (5)	2.53 (5)	−0.19 (4)	0.77 (4)	−0.28 (4)
O(9)	0.3425 (1)	−0.2097 (2)	−0.1708 (1)	1.91 (5)	1.89 (5)	3.32 (5)	0.07 (4)	1.18 (4)	−0.57 (5)
O(11)	0.5508 (2)	−0.0474 (2)	−0.2263 (2)	2.25 (5)	2.82 (5)	4.92 (7)	−0.32 (5)	1.99 (5)	−0.74 (6)
O(12)	0.6428 (1)	0.2096 (2)	−0.1882 (1)	1.56 (4)	3.11 (6)	4.05 (6)	−0.51 (5)	1.13 (5)	0.05 (5)
O(13)	0.0841 (1)	−0.0596 (2)	0.1937 (1)	1.91 (5)	2.65 (5)	2.32 (5)	0.43 (5)	0.34 (4)	0.01 (5)
N(1)	0.1784 (1)	0.1561 (2)	−0.0331 (1)	1.35 (5)	1.64 (5)	1.78 (5)	−0.11 (4)	0.46 (4)	0.02 (5)
N(4)	0.4182 (2)	0.3429 (2)	−0.0878 (1)	1.81 (6)	1.88 (6)	2.71 (6)	−0.41 (5)	0.42 (5)	−0.12 (5)
C(2)	0.2870 (2)	0.0774 (2)	−0.0901 (2)	1.53 (6)	1.47 (6)	1.43 (6)	0.06 (5)	0.19 (5)	0.11 (5)
C(3)	0.4081 (2)	0.1713 (2)	−0.1180 (2)	1.42 (6)	2.07 (7)	1.53 (6)	−0.01 (6)	0.19 (5)	0.18 (5)
C(5)	0.3109 (2)	0.4170 (2)	−0.0313 (2)	2.28 (7)	1.67 (7)	3.00 (8)	−0.26 (6)	0.54 (6)	−0.23 (6)
C(6)	0.1893 (2)	0.3246 (2)	−0.0033 (2)	1.98 (6)	1.78 (7)	2.30 (7)	0.05 (6)	0.61 (6)	−0.29 (6)
C(7)	0.2529 (2)	−0.1168 (2)	−0.1170 (2)	1.65 (6)	1.51 (6)	1.73 (6)	−0.16 (5)	0.26 (5)	−0.00 (5)
C(10)	0.5437 (2)	0.1098 (2)	−0.1819 (2)	1.64 (6)	2.23 (7)	2.01 (6)	0.06 (6)	0.45 (5)	0.35 (6)

atom	x	y	z	B, Å²	atom	x	y	z	B, Å²
H(5)	0.318 (4)	0.539 (4)	−0.009 (3)	5.1 (9)	H(132)	0.092 (4)	0.040 (4)	0.256 (3)	4.6 (8)
H(6)	0.107 (3)	0.380 (4)	0.038 (3)	4.1 (7)	H(11)	0.533 (3)	0.118 (4)	0.205 (2)	4.4 (6)
H(131)	0.156 (3)	−0.107 (4)	0.208 (3)	3.0 (6)					

(b) $[Co(C_4N_2COO)_2(H_2O)_2]\cdot 2H_2O$

atom	x	y	z	B_{11}	B_{22}	B_{33}	B_{12}	B_{13}	B_{23}
Co	0.0000 (0)	0.0000 (0)	0.0000 (0)	1.08 (2)	2.15 (2)	2.85 (2)	−0.06 (1)	0.00 (1)	−0.14 (1)
O(1)	0.2242 (2)	0.0978 (1)	−0.0114 (2)	1.49 (6)	2.35 (6)	3.17 (6)	−0.02 (5)	−0.07 (5)	0.38 (6)
O(2)	0.5230 (2)	0.1339 (1)	0.1036 (2)	1.40 (6)	2.89 (7)	4.66 (8)	−0.58 (6)	0.11 (6)	0.50 (7)
O(3)	0.9029 (2)	0.1021 (2)	0.1544 (2)	1.39 (6)	4.82 (9)	4.81 (8)	0.15 (7)	0.03 (6)	−2.32 (7)
O(4)	1.0929 (3)	0.1923 (2)	0.4234 (3)	3.34 (9)	5.50 (11)	5.07 (9)	1.48 (8)	−1.38 (8)	−2.29 (9)
N(1)	0.2134 (3)	−0.0548 (2)	0.1994 (2)	3.03 (8)	3.61 (8)	4.15 (8)	−0.00 (7)	0.47 (7)	−0.13 (8)
N(4)	0.5367 (3)	−0.1232 (2)	0.4140 (3)	3.06 (9)	2.76 (9)	3.02 (0)	0.51 (8)	−0.13 (8)	0.09 (8)
C(2)	0.3793 (3)	−0.0088 (2)	0.2054 (3)	1.46 (8)	2.05 (9)	2.43 (8)	−0.08 (7)	0.31 (7)	−0.34 (7)
C(3)	0.5410 (3)	−0.0438 (2)	0.3116 (3)	1.89 (9)	2.66 (9)	2.86 (10)	0.19 (9)	0.04 (7)	−0.39 (9)
C(5)	0.3702 (4)	−0.1659 (2)	0.4104 (3)	3.88 (12)	2.64 (10)	3.38 (10)	0.08 (10)	0.27 (9)	0.62 (9)
C(6)	0.2072 (4)	−0.1330 (2)	0.3030 (3)	2.83 (10)	2.44 (9)	3.69 (10)	−0.37 (9)	0.64 (9)	0.60 (9)
C(7)	0.3760 (3)	0.0814 (2)	0.0900 (3)	1.69 (8)	2.16 (9)	2.80 (8)	0.19 (7)	0.60 (7)	−0.30 (8)

atom	x	y	z	B, Å²	atom	x	y	z	B, Å²
H(3)	0.659 (4)	−0.012 (3)	0.308 (4)	3.1 (7)	H(32)	0.958 (5)	0.129 (3)	0.243 (4)	4.2 (9)
H(5)	0.363 (5)	−0.217 (3)	0.491 (4)	3.9 (8)	H(41)	1.051 (5)	0.244 (3)	0.476 (5)	5.1 (10)
H(6)	0.088 (5)	−0.163 (3)	0.310 (4)	3.5 (8)	H(42)	1.181 (5)	0.181 (3)	0.459 (4)	3.7 (8)
H(31)	0.805 (5)	0.112 (3)	0.151 (4)	2.9 (7)					

(c) $[Co(C_4N_2COO)_2(H_2O)_2]$

atom	x	y	z	B_{11}	B_{22}	B_{33}	B_{12}	B_{13}	B_{23}
Co	0.0000 (0)	0.0000 (0)	0.0000 (0)	1.36 (1)	0.93 (1)	1.77 (1)	0.153 (9)	0.67 (1)	0.140 (9)
O(1)	−0.2312 (2)	−0.0728 (1)	0.1274 (1)	1.69 (4)	1.22 (4)	2.25 (4)	0.27 (4)	0.92 (4)	0.18 (4)
O(2)	−0.3020 (2)	−0.2403 (1)	0.2353 (1)	2.64 (5)	1.90 (5)	2.72 (5)	0.18 (4)	1.51 (4)	0.60 (4)
O(3)	0.2955 (2)	0.0260 (1)	0.1643 (1)	1.63 (5)	1.83 (5)	2.48 (5)	0.17 (4)	0.39 (4)	−0.51 (4)
N(1)	0.1109 (3)	−0.1814 (1)	0.0030 (1)	1.40 (5)	1.23 (5)	1.76 (5)	0.08 (5)	0.47 (4)	−0.00 (5)
N(4)	0.2484 (3)	−0.4209 (1)	0.0506 (2)	2.82 (6)	1.46 (6)	3.53 (7)	0.62 (5)	1.20 (5)	0.13 (6)
C(2)	0.0051 (3)	−0.2468 (1)	0.0898 (2)	1.39 (6)	1.26 (6)	1.72 (6)	0.08 (5)	0.32 (5)	0.08 (5)
C(3)	0.0743 (4)	−0.3666 (2)	0.1118 (2)	2.52 (7)	1.43 (7)	2.75 (7)	0.20 (6)	1.12 (6)	0.31 (6)
C(5)	0.3488 (4)	−0.3546 (2)	−0.0363 (2)	2.05 (7)	1.91 (7)	2.66 (7)	0.48 (6)	0.83 (6)	−0.19 (6)
C(6)	0.2805 (3)	−0.2358 (2)	−0.0606 (2)	1.73 (6)	1.73 (7)	2.03 (6)	0.06 (6)	0.75 (5)	−0.04 (6)
C(7)	−0.1917 (3)	−0.1834 (1)	0.1586 (2)	1.38 (6)	1.43 (6)	1.62 (6)	−0.01 (5)	0.29 (5)	−0.01 (5)

atom	x	y	z	B, Å²	atom	x	y	z	B, Å²
H(3)	−0.008 (3)	−0.415 (2)	0.172 (2)	2.2 (4)	H(10)	0.426 (4)	−0.010 (1)	0.166 (2)	1.9 (4)
H(5)	0.483 (4)	−0.390 (2)	−0.081 (2)	3.0 (5)	H(20)	0.310 (5)	0.087 (2)	0.194 (2)	4.0 (5)
H(6)	0.351 (3)	−0.190 (2)	−0.124 (2)	1.6 (4)					

[a] The form of the anisotropic thermal parameter is $\exp[-(B_{11}a^{*2}h^2 + B_{22}b^{*2}k^2 + B_{33}c^{*2}l^2)/4 + (B_{12}a^*b^*hk + B_{13}a^*c^*hl + B_{23}b^*c^*kl)/2]$.

In $[Co(pzCOO)_2(H_2O)_2]\cdot 2H_2O$, both coordinated and the uncoordinated water molecules are involved in a three-dimensional hydrogen-bonded network. The coordinated carboxylate oxygens are not involved. Chains parallel to the *a* axis are joined by O(2)–H(31)–O(3) linkages, involving the coordinated water molecules. Hydrogen bonding involving the uncoordinated water molecule completes a three-dimensional network. This network is a suitable magnetic-exchange pathway, but the linkage is less direct than in $[Co(pzCOO)_2(H_2O)_2]$ because there are more intervening bonds between adjacent metal atoms. The most direct linkage for magentic-exchange interactions in $[Co(pzCOO)_2(H_2O)_2]\cdot 2H_2O$ is again along the *a* axis because this is the only direction in which the uncoordinated water molecule is not part of the pathway.

The ligand environment about the metal atom is a distorted octahedron in each case. The largest single contribution to the distortion is the O–Co–N angle required at the metal atom by the bidentate ligand: 77.6 (1), 78.0 (1), and 78.8 (1)° in $[Co(pz(COO)COOH)_2(H_2O)_2]$, $[Co(pzCOO)_2(H_2O)_2]\cdot 2H_2O$,

Table II. Bond Lengths and Nearest Intermolecular Contacts (Å)

(a) $[Co(C_4N_2(COO)COOH)_2(H_2O)_2]$			
Co-N(1)	2.109 (1)	C(7)-O(9)	1.253 (1)
Co-O(8)	2.057 (1)	C(10)-O(11)	1.294 (2)
Co-O(13)	2.123 (1)	C(10)-O(12)	1.212 (1)
N(1)-C(2)	1.349 (1)	C(5)-H(5)	0.97 (2)
N(1)-C(6)	1.326 (1)	C(6)-H(6)	0.99 (2)
C(2)-C(3)	1.390 (2)	O(13)-H(131)	0.78 (2)
C(2)-C(7)	1.548 (2)	O(13)-H(132)	0.99 (2)
C(3)-N(4)	1.358 (2)	O(12)-O(13)	2.817 (1)[a]
C(3)-C(10)	1.537 (1)	O(12)-O(13)	2.984 (1)[b]
N(4)-C(5)	1.317 (2)	Co-Co	7.692[c]
C(5)-C(6)	1.389 (2)	Co-Co	7.732[d]
C(7)-O(8)	1.245 (1)	Co-Co	8.081[e]
(b) $[Co(C_4N_2COO)_2(H_2O)_2]\cdot 2H_2O$			
Co-O(1)	2.084 (1)	C(6)-H(6)	0.96 (4)
Co-O(3)	2.068 (1)	N(1)-C(6)	1.339 (2)
Co-N(1)	2.135 (1)	C(2)-C(3)	1.387 (2)
O(1)-C(7)	1.255 (2)	C(2)-C(7)	1.510 (2)
O(2)-C(7)	1.253 (2)	C(3)-N(4)	1.341 (2)
N(1)-C(2)	1.337 (2)	N(4)-C(5)	1.325 (2)
O(3)-H(31)	0.71 (2)	C(5)-C(6)	1.389 (2)
O(3)-H(32)	0.83 (2)	O(2)-O(3)	2.732 (1)
O(4)-H(41)	0.89 (2)	O(3)-O(4)	2.635 (1)
O(4)-H(42)	0.66 (2)	O(2)-O(4)	2.815 (1)
C(3)-H(3)	0.96 (4)	O(4)-N(4)	2.885 (2)
C(5)-H(5)	0.95 (4)		
(c) $[Co(C_4N_2COO)_2(H_2O)_2]$			
Co-O(1)	2.093 (1)	N(4)-C(5)	1.335 (1)
Co-O(3)	2.117 (1)	C(5)-C(6)	1.383 (1)
Co-N(1)	2.102 (1)	O(3)-H(10)	0.79 (1)
O(1)-C(7)	1.282 (1)	O(3)-H(20)	0.74 (1)
O(2)-C(7)	1.230 (1)	O(3)-H(3)	0.98 (1)
N(1)-C(2)	1.342 (1)	C(5)-H(5)	0.98 (1)
N(1)-C(6)	1.336 (1)	C(6)-H(6)	0.95 (1)
C(2)-C(3)	1.391 (1)	O(1)-O(3)	2.801 (1)
C(2)-C(7)	1.520 (1)	O(2)-O(3)	2.800 (1)
C(3)-N(4)	1.338 (1)		

[a] Intermolecular H-bonding distance. [b] Intramolecular H-bonding distance. [c] $x, y \pm 1, z$. [d] $\pm(x + 1/2, y \pm 1/2, z + 1/2)$. [e] $\pm(x + 1/2, y \pm 1/2, z - 1/2)$.

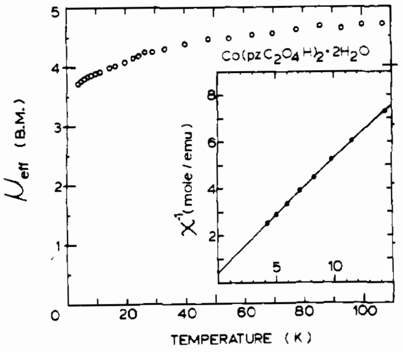

Figure 6. Low-temperature magnetic properties of $[Co(pz(COO)COOH)_2(H_2O)_2]$.

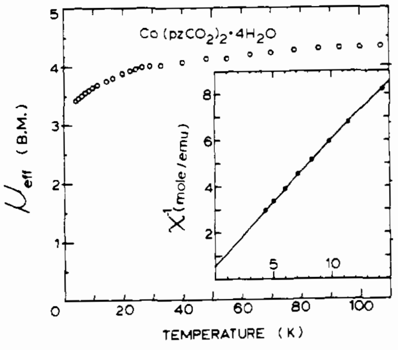

Figure 7. Low-temperature magnetic properties of $[Co(pzCOO)_2(H_2O)_2]\cdot 2H_2O$.

Table III. Bond Angles (Deg)

(a) $[Co(C_4N_2(COO)COOH)_2(H_2O)_2]$			
N(1)-Co-O(8)	77.6 (1)	C(3)-N(4)-C(5)	118.3 (1)
N(1)-Co-O(8′)	102.4 (1)	N(4)-C(5)-C(6)	121.8 (1)
N(1)-Co-O(13)	89.2 (1)	N(1)-C(6)-C(5)	120.3 (1)
O(8)-Co-O(13)	88.2 (1)	C(2)-C(7)-O(8)	117.4 (1)
Co-N(1)-C(2)	115.9 (1)	C(2)-C(7)-O(9)	119.3 (1)
Co-N(1)-C(6)	124.9 (1)	O(8)-C(7)-O(9)	123.3 (1)
N(1)-C(2)-C(3)	120.0 (1)	C(3)-C(10)-O(11)	119.7 (1)
N(1)-C(2)-C(7)	111.7 (1)	C(3)-C(10)-O(12)	119.1 (1)
C(3)-C(2)-C(7)	128.9 (1)	O(11)-C(10)-O(12)	121.2 (1)
C(2)-C(3)-N(4)	120.4 (1)	O(8)-Co-O(8′)	180
C(2)-C(3)-C(10)	129.4 (1)	O(13)-Co-O(13′)	180
N(4)-C(3)-C(10)	110.2 (1)	N(1)-Co-N(1′)	180
(b) $[Co(C_4N_2COO)_2(H_2O)_2]\cdot 2H_2O$			
O(1)-Co-O(1′)	180	N(1)-C(2)-C(3)	120.8 (2)
O(1)-Co-O(3)	90.3 (1)	N(1)-C(2)-C(7)	115.5 (2)
O(1)-Co-N(1)	78.0 (1)	C(3)-C(2)-C(7)	123.7 (2)
O(3)-Co-O(3′)	180	N(4)-C(3)-C(2)	121.7 (2)
O(3)-Co-N(1)	91.4 (1)	C(3)-N(4)-C(5)	116.8 (2)
N(1)-Co-N(1′)	180	N(4)-C(5)-C(6)	122.4 (2)
Co-O(1)-C(7)	116.8 (1)	N(1)-C(6)-C(5)	120.4 (2)
Co-N(1)-C(2)	112.4 (1)	O(1)-C(7)-O(2)	125.4 (2)
Co-N(1)-C(6)	129.3 (1)	O(1)-C(7)-C(2)	116.7 (2)
C(2)-N(1)-C(6)	118.0 (1)	O(2)-C(7)-C(2)	117.9 (2)
(c) $[Co(C_4N_2COO)_2(H_2O)_2]$			
O(1)-Co-O(1′)	180	N(1)-C(2)-C(3)	120.2 (1)
O(1)-Co-O(3)	88.6 (1)	N(1)-C(2)-C(7)	116.5 (1)
O(1)-Co-N(1′)	78.8 (1)	C(3)-C(2)-C(7)	123.3 (1)
O(3)-Co-O(3′)	180	N(4)-C(3)-C(2)	122.5 (1)
O(3)-Co-N(1′)	87.4 (1)	C(3)-N(4)-C(5)	116.2 (1)
N(1)-Co-N(1′)	180	N(4)-C(5)-C(6)	122.1 (1)
Co-O(1)-C(7)	116.3 (1)	N(1)-C(6)-C(5)	121.3 (1)
Co-N(1)-C(2)	112.8 (1)	O(1)-C(7)-O(2)	125.6 (1)
Co-N(1)-C(6)	129.4 (1)	O(1)-C(7)-C(2)	115.1 (1)
C(2)-N(1)-C(6)	117.6 (1)	O(2)-C(7)-C(2)	119.3 (1)

Table IV. Average Metal-Ligand Distances (Å)

	$[Co(pyz(COO)COOH)_2(H_2O)_2]$	$[Co(pyzCOO)_2(H_2O)_2]\cdot 2H_2O$	$[Co(pyzCOO)(H_2O)_2]$
Co-N	2.109	2.135	2.102
⟨Co-O⟩	2.090	2.076	2.105
⟨Co-lig⟩	2.096	2.096	2.104

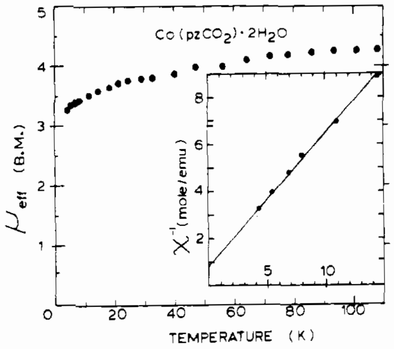

Figure 8. Low-temperature magnetic properties of $[Co(pzCOO)_2(H_2O)_2]$.

and $[Co(pzCOO)_2(H_2O)_2]$, respectively. Consequently, the equatorial planes of ligand donor atoms deviate from being at right angles as required for a regular octahedron: the plane consisting of the two nitrogen and two water oxygen donors make angles of 77.7, 78.2, and 78.9° with the plane of four oxygen donors in $[Co(pz(COO)COOH)_2(H_2O)_2]$, $[Co(pzCOO)_2(H_2O)_2]\cdot 2H_2O$, and $[Co(pzCOO)_2(H_2O)_2]$, respectively.

High-precision magnetic measurements were carried out in order to determine whether magnetic-exchange interactions are present in the complexes. The effective magnetic moment ($\mu_{eff} = (8\chi T)^{1/2}$) is plotted as a function of temperature in Figures 6–8, including an expanded region plot of χ^{-1} vs. T

Table V. Curie-Weiss Parameters for the Compounds (4-15 K)

compd	g	Θ/K	TIP/emu mol^{-1}
$[Co(pz(COO)COOH)_2(H_2O)_2]$	4.60	−0.78	0.006
$[Co(pzCOO)_2(H_2O)_2]\cdot 2H_2O$	4.31	−1.00	0.008
$[Co(pzCOO)_2(H_2O)_2]$	4.17	−1.10	0.006

from 4 to 25 K. The data were analyzed in the low-temperature region (4–24 K) with the Curie–Weiss law plus a correction for temperature-independent paramagnetism (TIP). The equation used is

$$\chi = \frac{Ng^2\mu_\beta^2 S(S+1)}{3k(T-\Theta)} + \text{TIP} \tag{1}$$

Due to effects of spin–orbit coupling and distortion from octahedral symmetry, cobalt(II) has a low-lying anisotropic Kramers doublet. Its magnetic behavior may be approximated at low temperatures with an effective spin $S = {}^1/_2$ in eq 1. The lowest lying excited magnetic state is usually at least some 100 cm^{-1} above the doublet and is therefore appreciably depopulated at lower temperatures ($T < 25$ K).[34] However, the magnetic excited states necessitate the inclusion of a TIP term due to coupling with the ground state.[35]

The parameters obtained from the fits of the data to eq 1 are listed in Table V. The negative value for the Θ term may only be explained by antiferromagnetically coupled monomeric units since the Kramers doublet may not be further split.

Pyrazine has been shown to be an effective magnetic bridge in many magnetic systems. However, in this case, hydrogen bonding is required to propagate magnetic superexchange. These complexes are excellent candidates for investigating the magnetic properties of chemically similar materials with different magnetic-superexchange pathways. From the magnetic parameters, the critical region is expected to occur below 1 K in each of the complexes. Further measurements below 1 K will be required for information on the critical regions.

Acknowledgment. Support received under NSF Grant No. CHE77-01372 is gratefully acknowledged.

Registry No. $Co(pz(COO)COOH)_2(H_2O)_2$, 75658-52-5; $[Co(pzCOO)_2(H_2O)_2]\cdot 2H_2O$, 75600-06-5; $Co(pzCOO)_2(H_2O)_2$, 74184-89-7.

Supplementary Material Available: A listing of least-squares planes for $[Co(pz(COO)_2)_2]$ and tables of observed and calculated structure factors for $[Co(pz(COO)COOH)_2(H_2O)]$, $[Co(pzCOO)_2(H_2O)_2]\cdot 2H_2O$, and $[Co(pzCOO)_2(H_2O)_2]$ (19 pages). Ordering information is given on any current masthead page.

---

(34) Carlin, R. J; O'Connor, C. J.; Bhatia, S. N. *J. Am. Chem. Soc.* **1976**, *98*, 685.

(35) Leask, M. J. M.; Wolf, W. P. *Proc. Phys. Soc., London* **1963**, *81*, 252.

Contribution from the Materials and Molecular Research Division, Lawrence Berkeley Laboratory,
and the Department of Chemistry, University of California, Berkeley, California 94720

Divalent Lanthanide Chemistry. Preparation of Some Four- and Six-Coordinate Bis[(trimethylsilyl)amido] Complexes of Europium(II). Crystal Structure of Bis[bis(trimethylsilyl)amido]bis(1,2-dimethoxyethane)europium(II)

T. DON TILLEY, ALLAN ZALKIN,* RICHARD A. ANDERSEN, and DAVID H. TEMPLETON

Received June 11, 1980

The yellow, hydrocarbon-soluble, divalent derivatives of europium(II) of the type $[(Me_3Si)_2N]_2Eu(L)_2$, where L is tetrahydrofuran or 1,2-dimethoxyethane, and $[(Me_3Si)_2N]_2Eu(bpy)$ have been prepared. The crystal structure of $[(Me_3Si)_2N]_2Eu[MeOCH_2CH_2OMe]_2$ has been determined by single-crystal X-ray diffraction methods. The crystals are monoclinic, $C2/c$, with cell dimensions $a = 13.398$ (4) Å, $b = 17.454$ (6) Å, $c = 15.013$ (5) Å, $\beta = 92.91$ (3)°, and $V = 3506$ Å^3. For $Z = 4$, the calculated density is 1.24 g/cm^3. The structure was refined to a conventional R factor of 0.039 by using 2259 data where $F^2 > \sigma(F^2)$. The Eu(II) atom is hexacoordinate and bonded to two nitrogen atoms of the two bis(trimethylsilyl)amido groups and to four oxygen atoms of the 1,2-dimethoxyethane ligands. The molecule has C_2 symmetry. The Eu(II)–N bond distance is 2.530 (4) Å and the Eu(II)–O distances are 2.634 (4) and 2.756 (4) Å. The ethane carbon atoms in the 1,2-dimethoxyethane ligand are disordered.

Introduction

Compounds of europium in its divalent oxidation state are rather less well characterized than are those of the more common trivalent oxidation state. Some simple halides, chalcogenides, and organometallic compounds have been prepared, and their physical properties have been studied.[1,2] These compounds are generally insoluble, and their solid-state structures are coordination polymers with high coordination number metal atoms. One way to prevent polymer formation is with use of sterically voluminous ligands, one such ligand being the bis(trimethylsilyl)amido ligand, $(Me_3Si)_2N$. This ligand has been used to prepare low coordination number complexes of most elements in the periodic table.[3,4] Even the trivalent uranium derivative, $[(Me_3Si)_2N]_3U$, is monomeric and three-coordinate, a most unusual constitution for this large actinide ion.[5]

In this paper we describe the synthesis of some coordination complexes of bis[bis(trimethylsilyl)amido]europium(II) and the crystal structure of one of them, viz., $[(Me_3Si)_2N]_2Eu(dme)_2$, where dme is the chelating ether 1,2-dimethoxyethane. This is the only monomeric, molecular compound of Eu(II)

---

* To whom correspondence should be addressed at the Lawrence Berkeley Laboratory.

(1) Johnson, D. A. *Adv. Inorg. Chem. Radiochem.* **1977**, *20*, 1.

(2) Marks, T. J. *Prog. Inorg. Chem.* **1978**, *24*, 51.

(3) Eller, P. G.; Bradley, D. C.; Hursthouse, M. B.; Meek, D. W. *Coord. Chem. Rev.* **1977**, *24*, 1.

(4) Harris, D. H.; Lappert, M. F. *J. Organomet. Chem. Libr.* **1976**, *2*, 13.

(5) Andersen, R. A. *Inorg. Chem.* **1979**, *18*, 1507.

0020-1669/81/1320-0551$01.00/0